

This work was written as part of one of the author's official duties as an Employee of the United States Government and is therefore a work of the United States Government. In accordance with 17 U.S.C. 105, no copyright protection is available for such works under U.S. Law.

Public Domain Mark 1.0

<https://creativecommons.org/publicdomain/mark/1.0/>

Access to this work was provided by the University of Maryland, Baltimore County (UMBC) ScholarWorks@UMBC digital repository on the Maryland Shared Open Access (MD-SOAR) platform.

Please provide feedback

Please support the ScholarWorks@UMBC repository by emailing scholarworks-group@umbc.edu and telling us what having access to this work means to you and why it's important to you. Thank you.

Erythemally weighted UV trends over northern latitudes derived from Nimbus 7 TOMS measurements

J. R. Ziemke¹

Software Corporation of America, Beltsville, Maryland

S. Chandra and J. Herman

NASA Goddard Space Flight Center, Greenbelt, Maryland

C. Varotsos

Department of Applied Physics, University of Athens, Athens, Greece

Abstract. This study examines the distribution of long-term trends in ground level erythemally weighted ultraviolet (UV) exposures in the northern latitudes for the period 1979–1991 using measurements from the Nimbus 7 Total Ozone Mapping Spectrometer (TOMS) instrument. A new erythemal UV data set (now available to the public via World Wide Web) was produced recently by NASA and has been tested by NASA at the Goddard Space Flight Center against a previous NASA erythemal UV product, which was used in a former study that included similar adjustments for aerosols and clouds but not aerosol absorption. Zonal mean erythemal UV data from both products show similar, ~3–7% per decade, increases in the midlatitudes to high latitudes. The detection of regional patterns in trends in erythemal UV favors summer months when surface UV is strongest and noise factors such as clouds and aerosols are not as influential. Analysis of the zonal patterns in trends around summer months indicates that most of the regional increases (exceeding 6% per decade) in the Northern Hemisphere in the latitude range 30°N–40°N originate from the Pacific and Atlantic oceanic regions. Increases (also exceeding 6% per decade) in latitudes 40°–60°N appear to originate from the North American and Asian continents and also central Europe. Trends over the east Asian continent in high latitudes indicate increases exceeding 10% per decade for May–August. The important conclusion is that positive trends in the northern subtropical latitudes originate mostly over oceanic regions, whereas positive trends at higher latitudes originate mostly over landmasses. Some of the increases in erythemal UV over central Europe and the east Asian continent in summer months can be attributed to decadal decreases in cloudiness for the 1979–1991 time period.

1. Introduction

Since the discovery of the Southern Hemisphere (SH) ozone hole in 1985 [Farman *et al.*, 1985], there has been great concern among scientists and the general public regarding the impact of stratospheric O₃ loss on increases in surface ultraviolet (UV) radiation. These increases in UV primarily involve two biologically important wavelength bands. The first is the ultraviolet B (UV-B) band, which represents solar radiation with wavelengths between 290 and 320 nm and is strongly attenuated by ozone in the stratosphere. UV radiation with wavelengths 320–400 nm corresponds to the UV-A band and is weakly absorbed by stratospheric ozone. Erythemally weighted UV represents an effective biological weighting of radiation involving these wavelength bands [e.g., Tsay and Stamnes, 1992], with larger UV weights for longer wavelengths compared to either DNA or plant action spectra.

The attenuation of UV flux through the atmosphere is highly dependent upon wavelength with shorter UV wavelength radiation absorbed more strongly by stratospheric O₃ [e.g., Madronich, 1993]. There have been many studies describing how ground level UV-B and total ozone column (TOC) are inversely related [e.g., McKenzie *et al.*, 1992; Madronich, 1993; Bojkov *et al.*, 1995; Fioletov *et al.*, 1997; Zerefos *et al.*, 1997]. The basic relation between trends in TOC and wavelength dependent surface UV can be understood using a simple model that relates changes between these parameters. For a clear atmosphere the attenuation of the primary beam of UV radiance can be approximated by (I_0 = const; α , attenuation factor; Ω , total column O₃; and θ , solar zenith angle (angle between the Sun and the vertical))

$$I = I_0 \cos \theta e^{-\alpha \Omega \sec \theta}. \quad (1)$$

It follows from (1) that small differential change in I caused by small differential change in Ω is given by

$$\frac{dI}{I} = -(\alpha \Omega \sec \theta) \frac{d\Omega}{\Omega}. \quad (2)$$

Since changes in the scattered radiation are proportional to changes in the primary beam, (2) can be used to approximate

¹Also at NASA Goddard Space Flight Center, Greenbelt, Maryland.

relative changes in surface UV exposures. The quantity $\alpha\Omega \sec \theta$ in (2) is the radiation amplification factor (RAF), and it is this important quantity that relates trends in Ω with trends in surface UV. For erythemally weighted UV with a solar zenith angle of zero the mean value for the RAF is around 1.1–1.2. Thus, for a trend of -1% per decade in Ω we would expect around 1.1–1.2% per decade increase in surface erythemal UV. For moderate to short UV-B wavelength radiation the UV trends are larger because of the strong wavelength dependence of α . A first-order calculation using (2) with $\theta = 0$ indicates that the RAF is around 11 at 290 nm, suggesting $\sim +11\%$ per decade trend in UV for a -1% per decade trend in Ω . Hence, even small negative trends of a few percent per decade in Ω can produce much larger positive trends in surface UV at short UV-B wavelengths. We note that the RAF and its effect becomes larger for $\theta \neq 0$ in (2) (characteristic of middle and higher latitudes).

The above model (1), relating TOC with surface UV, is only a first-order approximation. Variability in ground level UV depends on several parameters besides just ozone and solar zenith angle, including transient cloud cover amount, surface albedo, and aerosols (largely dust, smoke, and urban pollution). The variability in TOC is also coupled with dynamical transport in the stratosphere [e.g., Schoeberl and Krueger, 1983; Mote et al., 1991; Salby and Callaghan, 1993; Randel and Cobb, 1994; Hood and Zaff, 1995; Chandra et al., 1996; McCormack and Hood, 1997; Hood et al., 1997; Ziemke et al., 1997]. Because of the natural variabilities present in TOC it is difficult to isolate anthropogenic ozone depletion (and resulting surface UV increases) from nonanthropogenic causes [e.g., Bruhl and Crutzen, 1989; Blumthaler and Ambach, 1990; Lubin and Jensen, 1995; Eck et al., 1995; von der Gathen et al., 1995; Rex et al., 1998]. The problem of isolating anthropogenic increases in surface UV becomes especially evident in regions where variations in TOC are strong. Chandra et al. [1996] suggested that in midlatitudes some of the observed trends in TOC may be manifestations of a relatively large interannual variability in TOC during winter-spring months and the length of the TOC time series. Because interannual variability in ozone is caused mainly by dynamical factors such as the quasi-biennial oscillation (QBO), El Niño–Southern Oscillation, episodic medium-scale waves (4000–8000 km zonal wavelengths in midlatitudes), and planetary-scale waves (wavelengths greater than 8000 km in midlatitudes to high latitudes) [e.g., Niu et al., 1992; Hood and Zaff, 1995; Chandra et al., 1996; McCormack and Hood, 1997; Ziemke et al., 1997], the trends in TOC and UV will likely vary significantly with latitude and longitude. Chandra et al. [1996] found that by using microwave sounding unit channel 4 (MSU4) deseasonalized temperature as an index of local dynamical variability in trend calculations, the large negative trends in midlatitude TOC are reduced in magnitude by 1–3% per decade. These reductions in TOC trends are attributed to trends present in lower stratospheric temperature.

There have been several studies that investigated trends in surface UV using ground-based measurements. One of these studies was by Blumthaler and Ambach [1990], who found a $+10\%$ per decade increase in clear sky erythemal UV at a location (altitude ~ 3.6 km) in the Swiss Alps for the time period 1981–1989. (This time period coincides with the 1979–1991 period chosen for this study.) In more recent years, Zerefos et al. [1997] found increases in 305 nm UV of around 2.7% per year for the time period 1991–1996 at Thessalonika, Greece (41°N , 23°E). Zerefos et al. [1998] showed increases in

305 nm UV of around $+10\%$ per decade for 1991–1997. Another recent ground-based study by McKenzie et al. [1999] indicated that in New Zealand (45°S) in the summer of 1998–1999, erythemal UV radiation was around $+12\%$ more than in the first years of the decade. It is indicated from ground-based measurements that surface UV has continued to increase significantly throughout the 1990s in both hemispheres.

Ground-based measurements are very important, but they represent localized monitoring of long-term changes in surface UV. Global monitoring of surface UV requires satellite measurements such as those from the Total Ozone Mapping Spectrometer (TOMS) instrument onboard the Nimbus 7 satellite [Herman et al., 1996]. The study by Herman et al. [1996] indicated measured increases ($\sim +4$ to $+8\%$ per decade) in zonal mean erythemally weighted UV in the midlatitudes to high latitudes of both hemispheres for the 1979–1992 time period.

The purpose of this study is to investigate the horizontal distribution of erythemal UV trends in the Northern Hemisphere (NH) derived from 1979 to 1991 Nimbus 7 TOMS measurements. The erythemal UV data represent daily UV exposures derived by time integration of erythemally weighted UV irradiances over the day as discussed by Herman et al. [1999].

This paper is comprised of five remaining sections. Sections 2–4 discuss data and analysis, discuss examples of erythemal UV time series, and compare the zonal mean erythemal UV data with that of an earlier study by Herman et al. [1996]. Section 5 discusses in detail the pattern distributions of trends in the northern hemisphere and, finally, section 6 provides a summary.

2. Data and Analyses

The new erythemal UV data include both aerosol scattering and improved cloud corrections and a new adjustment scheme for absorbing aerosols [Herman et al., 1999]. We have chosen the 1979–1991 time period because after 1991 and until the failure of the TOMS instrument in May 1993, TOC values in midlatitudes were affected by the Mount Pinatubo eruption [e.g., Gleason et al., 1993]. In this respect, Chandra [1993] and Randel and Cobb [1994] suggested that the inclusion of the post-Pinatubo period causes TOC trends to be more negative by 0.2–1.2% per decade. We note that more current TOMS measurements exist for studying long-term variability including Meteor 3 TOMS (1991–1994) and Earth Probe (EP) TOMS data (late July 1996 to the present). However, because of instrument calibration differences, derived trends in either TOC or surface UV are less certain when these different instruments are combined to obtain a longer time record. For this reason and also because the 1979–1991 time period corresponds to one complete peak-to-peak cycle in solar UV (important for regression analysis), we have opted to include only the Nimbus 7 data.

Our study compares trends in erythemal UV with trends derived from the erythemal UV data used by Herman et al. [1996]. We note that the erythemal UV data in that investigation also corrected for aerosols and clouds but not absorbing aerosols. Trends in erythemal UV are calculated using an extended linear regression model similar to the one used by Ziemke et al. [1997] ($t = 0, 1, \dots, 155$, corresponding to January 1979 through December 1991):

$$UV(t) = A(t) + B(t)t + C(t)QBO(t) + D(t)S(t) + E(t)P(t) + R(t), \quad (3)$$

where $A(t)$ represents the 12-month seasonal fit, $B(t)$ is the 12-month seasonal trend coefficient, $R(t)$ represents the residual error time series, and $C(t)$, $D(t)$, and $E(t)$ are 12-month coefficients corresponding to UV-driving time series $QBO(t)$ (nonlagged empirical orthogonal function winds as used by Ziemke et al. [1997]), $S(t)$ is $F_{10.7}$ solar UV proxy, and $P(t)$ is an optional proxy. For $S(t)$ in (3), Ottawa 10.7 cm solar flux ($F_{10.7}$) monthly time series was incorporated. For $P(t)$ we have used deseasonalized and linearly detrended (over the 1979–1991 time period) microwave sounding unit channel 4 (MSU4) temperature data from the National Oceanic and Atmospheric Administration. Temperatures from MSU4 are weighted mean values centered at around 90 hPa in the stratosphere (half-vertical weighting response close to 40 and 150 hPa). As shown by both Chandra et al. [1996] and Ziemke et al. [1997], the inclusion of MSU4 data in (3) for total ozone improves statistics by reducing the residual term $R(t)$. It is expected that MSU4 data also improve statistics for erythemal UV (see time series in section 3). The seasonal coefficients are all given by the harmonic expansion $c_0 + \sum_{j=1}^M [c_j \cos(2\pi jt/12) + s_j \sin(2\pi jt/12)]$, where c_j and s_j are constants. The values of M for $A(t)$, $B(t)$, $C(t)$, $D(t)$, and $E(t)$ are 4, 3, 2, 2, and 2, respectively (a total of 31 constants).

Trends derived from (3) also include additional 1% per decade local measurement uncertainties present in version 7 TOMS TOC, which for erythemal UV translates to 1.0–1.3% per decade throughout middle and higher latitudes (largest errors in winter months). For simplicity we have opted to include additional 1.3% per decade uncertainties in derived erythemal UV trends everywhere in our analyses. Prior to trend analysis, all data were averaged monthly and binned to a $5^\circ \times 15^\circ$ (latitude \times longitude) gridding. The seasonal coefficients in (3) were derived using standard least squares. To compute uncertainties in these seasonal coefficients, a direct method was invoked (this was not a Monte Carlo iterative method and did not model $R(t)$ with autoregression, etc.). A multivariate statistical analysis was used to derive coefficient errors for each time series. From the calculated covariance matrix, cross-covariance values for the constants in coefficient $A(t)$ (same for the other seasonal coefficients) provided the coefficient variances. These coefficient variances included additional seasonal modulation using the seasonal cycles present in the residual $R(t)$. The coefficient uncertainties with this method were previously compared (results not shown) with the Monte Carlo results of Ziemke et al. [1997], showing essentially the same 2σ significance level and confidence interval values. We refer the reader to *Stratospheric Processes and Their Role in Climate* [1998], which discusses several different statistical trend models.

3. Erythemal UV Time Series

As examples of erythemal UV time series, we plot data from several regions that exhibit statistically significant increases in surface erythemal UV over 1979–1991. Figure 1 compares deseasonalized time series of erythemal UV (solid line) and MSU4 brightness temperature (dotted line) over central Europe (Figure 1a) and the Mediterranean region (Figure 1b). For purposes of comparison with background erythemal UV amounts, climatological values of erythemal UV for these two

regions are provided in Table 1. The erythemal UV and MSU4 time series in Figure 1 indicate negative correlations, which are caused primarily by interannual changes in dynamical transport of stratospheric ozone [e.g., Chandra et al., 1996; Ziemke et al., 1997]. The stronger negative correlation for the Mediterranean region reflects dynamical transport of lower stratospheric ozone caused by midlatitude synoptic-scale baroclinic events [e.g., Schubert and Munteanu, 1988]. For central Europe, which is farther to the north, the influence of baroclinic waves on surface erythemal UV is less. Also plotted in Figure 1 are simple regression line fits for both erythemal UV time series, indicating statistically significant increases in erythemal UV of around 96 and 118 J m^{-2} per decade (6.2 and 4.5% per decade) over central Europe and the Mediterranean region, respectively.

For completeness, Figure 2 plots the erythemal UV time series from Figure 1 against TOMS total column ozone measurements. We note that the positive trends in erythemal UV in Figures 1 and 2 are associated with negative trends in TOC and MSU4 temperatures (line fits not shown in Figures 1 and 2). This implies stratospheric radiative effects (depletion of ozone reduces temperature) and/or decadal changes in dynamical transport. While radiative effects will be present on such a long-time scale, there has previously been shown evidence that decadal changes in dynamical transport have had a role in observed negative trends in TOC over NH midlatitudes [e.g., Hood and Zaff, 1995; Chandra et al., 1996; Hood et al., 1997; Ziemke et al., 1997].

Figure 3 (similar to Figure 1) plots deseasonalized erythemal UV and MSU4 time series for the oceanic north Atlantic (Figure 3a) and eastern Russia (Figure 3b). Erythemal UV time series indicate statistically significant increases in erythemal UV of around 166 and 11 J m^{-2} per decade (5.7 and 8.6% per decade) for the north Atlantic and eastern Russia region, respectively. The influence of baroclinic waves on erythemal UV is apparent for the north Atlantic but not eastern Russia. The latter, being at a much higher northern latitude, exhibits low erythemal UV even in summer months (see Table 2). For eastern Russia the MSU4 temperature time series shows several anomalous excursions (caused mostly by long planetary-scale wave events), but they occur during the winter and spring months when erythemal UV is very low. The result is that there is expected to be little correlation between erythemal UV and MSU4 temperatures. Although total ozone and MSU4 temperature are highly positively correlated (correlation $r = +0.83$) over eastern Russia (figure not shown), erythemal UV and MSU4 temperature are not.

The main conclusions from Figures 1–3 are (1) erythemal UV shows statistically significant positive trends for these regions, (2) interannual variabilities in erythemal UV in midlatitudes appear to be driven largely by baroclinic disturbances and to a lesser extent by planetary-scale wave events, and (3) erythemal UV in high latitudes shows little correlation with dynamical events in the stratosphere, primarily because these events occur during winter and spring when surface erythemal UV is very low.

4. Comparison Between Erythemal UV and Previous Erythemal UV Exposure Data From Nimbus 7 TOMS

Figure 4 shows annually averaged trends (using (3)) of zonal mean erythemal UV (solid line) and erythemal UV data used by Herman et al. [1996] (dotted line). In both data sets, trends

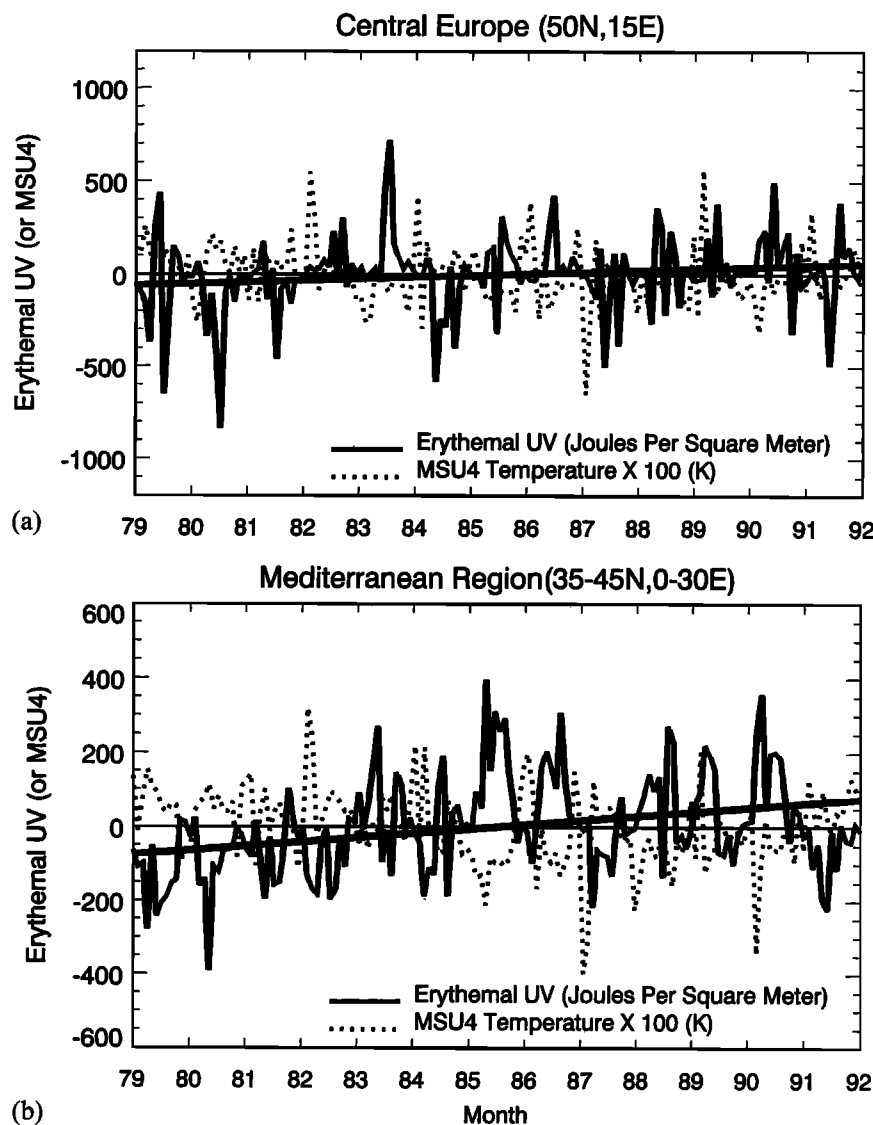


Figure 1. Deseasonalized Erythemal UV (solid) and deseasonalized MSU4 brightness temperature (dotted) time series over (a) central Europe and (b) the Mediterranean region for 1979–1991. Central Europe is defined by a $5^\circ \times 15^\circ$ region centered at 50°N , 15°E . The Mediterranean region is derived by averaging all data over area between latitudes $35^\circ\text{--}45^\circ\text{N}$ and longitudes $0^\circ\text{--}30^\circ\text{E}$. Also shown are regression line fits for both erythemal UV time series. For central Europe, the linear trend is 96 ± 86 (2σ) J m^{-2} or equivalently $6.2 \pm 5.6\%$ per decade. For the Mediterranean region, the trend is 118 ± 53 (2σ) J m^{-2} or equivalently $4.5 \pm 2.0\%$ per decade. Correlation between erythemal UV and MSU4 time series are (a) -0.32 and (b) -0.57 .

are essentially similar (within the 2σ uncertainties shown) and statistically significant in the middle to higher latitudes. These erythemal UV data show $\sim 3\text{--}7\%$ per decade increases in the middle and higher latitudes. Trends (although not statistically significant) for the previous UV data in the NH midlatitudes to high latitudes are smaller than the newer data. The cause for

these different trends reflects the new cloud transmission model used by *Herman et al.* [1999].

We note that the derived trends in Figure 4 for the previous erythemal UV data are essentially the same as the trends shown by *Herman et al.* [1996, Figure 2] but are not equivalent since that study included 1992 data, which makes only small

Table 1. Monthly Climatology (1979–1991) of Erythemal UV for the Central European and Mediterranean Regions

Region	Jan.	Feb.	March	April	May	June	July	Aug.	Sept.	Oct.	Nov.	Dec.
Central Europe	216	533	1050	1902	2818	3151	3277	2703	1696	827	302	112
Mediterranean	634	1053	1912	2974	3968	4849	5159	4427	3145	1761	869	553

Units Joules per square meter.

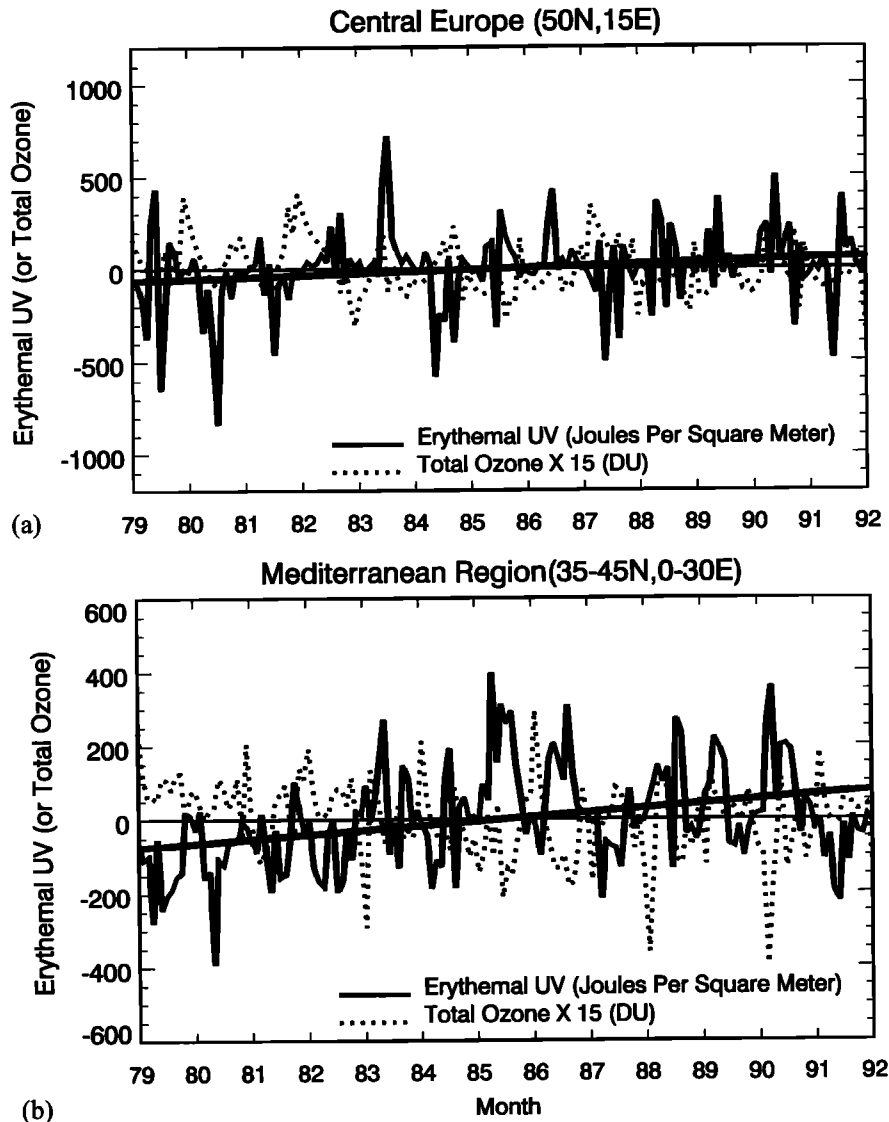


Figure 2. Same as Figure 1, except with the Total Ozone Mapping Spectrometer (TOMS) total column ozone in place of MSU4 brightness temperature. Correlation between erythemal UV and TOMS total ozone time series are (a) -0.14 and (b) -0.46 .

differences in trends, and also the trend model was slightly different (it did not include MSU4 data). Statistical uncertainties with the erythemal UV data appear to be smaller in middle and higher latitudes than uncertainties with the previous erythemal UV data.

5. The Distribution of Erythemal UV Trends in Summer Months

Figure 5 shows trends (units percent per decade) in zonal mean erythemal UV exposures for the latitude bands 30° – 40° N and 40° – 60° N. For completeness, Figure 6 plots these same trends but in physical units for exposure (trend units are J m^{-2} per decade). In physical units, largest statistically significant trends in Figure 6 occur in summertime, centered around the months of May–August. Summer months are expected to exhibit the largest physical trends and the best signal to noise for detecting regional patterns in trends. Figures 7 and 8 show the horizontal distribution of erythemal UV trends (units percent

per decade) for the months of May–August. The horizontal patterns in trends indicate that most of the increases (exceeding 6% per decade) in the latitude band 30° – 40° N originate from the Pacific (June–August) and Atlantic (May–August) oceanic regions. Increases (also exceeding 6% per decade) in the latitude band 40° – 60° N appear to originate mostly from the North American (July–August) and east Asian (May–August) continents and also central Europe (July–August). Trends over east Asia in high latitudes indicate increases exceeding 10% per decade. Decreases in cloudiness (J. R. Herman et al., manuscript in preparation, 1999) over central Europe and east Asia contribute to the positive trends observed in erythemal UV. These NH trends are comparable to SH trends over Australia ($\sim +10\%$ per decade) in summer months derived by Udelhofen et al. [1999] from the same erythemal UV data set used in this study. An important conclusion is that positive trends in erythemal UV in NH subtropical latitudes tend to originate mostly over oceanic regions whereas positive trends at higher latitudes originate mostly over land.

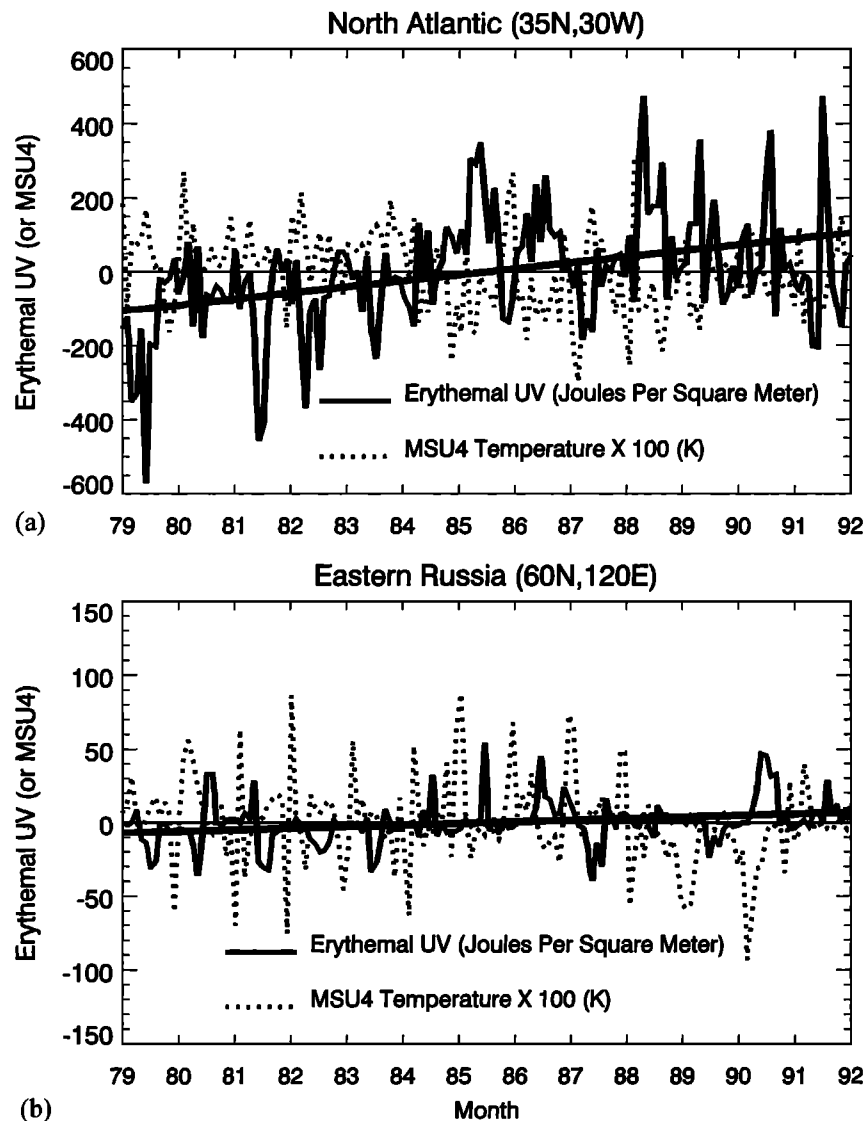


Figure 3. Same as Figure 1 except for (a) the North Atlantic and (b) Eastern Russia. The north Atlantic region is defined by a $5^\circ \times 15^\circ$ region centered at 35°N , 30°W . The eastern Russia region is defined by a $5^\circ \times 15^\circ$ region centered at 60°N , 120°E . For the north Atlantic, the linear trend is 166 ± 62 (2σ) J m^{-2} , or equivalently $5.7 \pm 2.1\%$ per decade. For the eastern Russia region, the trend is 11 ± 6 (2σ) J m^{-2} , or equivalently $8.6 \pm 4.8\%$ per decade. Correlation between erythemal UV and MSU4 time series are (a) -0.53 and (b) -0.17 .

6. Summary

This study has investigated trends in TOMS NH erythemal UV data for 1979–1991 (currently available via World Wide Web at <http://toms.gsfc.nasa.gov/>). Simple linear trend analysis of surface erythemal UV time series over central Europe and the Mediterranean region indicates increases of 96 and 118 J m^{-2} per decade (6.2 and 4.5% per decade), respectively. Sim-

ilar analyses for the oceanic north Atlantic and high-latitude east Asian continent show statistically significant increases of 166 and 11 J m^{-2} per decade (5.7 and 8.6% per decade), respectively. Interannual variabilities in erythemal UV in the midlatitudes appear to be driven largely by baroclinic disturbances. In the higher latitudes, erythemal UV shows little correlation with dynamical events in the stratosphere, primarily because the strong stratospheric disturbances occur in win-

Table 2. Monthly Climatology (1979–1991) of Erythemal UV for the North Atlantic and Eastern Russia Regions

Region	Jan.	Feb.	March	April	May	June	July	Aug.	Sept.	Oct.	Nov.	Dec.
North Atlantic	954	1491	2454	3420	4198	4797	5146	4760	3604	2223	1221	863
Eastern Russia	10	19	70	159	241	306	323	226	106	45	17	18

Units Joules per square meter.

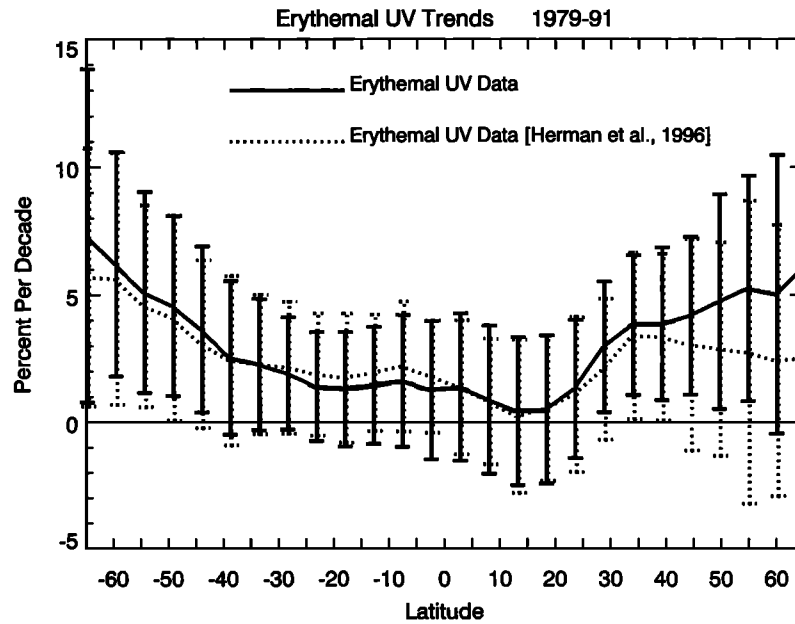


Figure 4. Annually averaged trends (units percent per decade) in global zonal-mean erythral UV exposure data (solid) and previous erythral UV exposure data (dotted, see text) for 1979–1991. Vertical bars denote $\pm 2\sigma$ uncertainties in trend coefficients.

ter and spring when the surface erythral UV is very low. Trends in zonally averaged erythral UV data were found to agree with trends derived from a previous TOMS erythral UV data product used in a previous study. (The previous data included similar adjustments for aerosols and clouds but not aerosol absorption.) Zonal mean erythral UV data from both products show ~ 3 – 7% per decade increases in the mid-latitudes to high latitudes. The detection of regional patterns in trends in erythral UV works best around summer months

when surface UV is strongest and noise factors (e.g., clouds, aerosols, etc.) are not as influential. Analysis of the horizontal patterns in erythral UV trends around summer months indicates that most of these increases (regionally exceeding 6% per decade) in the NH and in the latitude range 30° – 40° N originate from the Pacific and Atlantic oceanic regions. Increases (also exceeding 6% per decade) in latitudes 40° – 60° N appear to originate from the North American and Asian continents and also central Europe. Trends over the east Asian

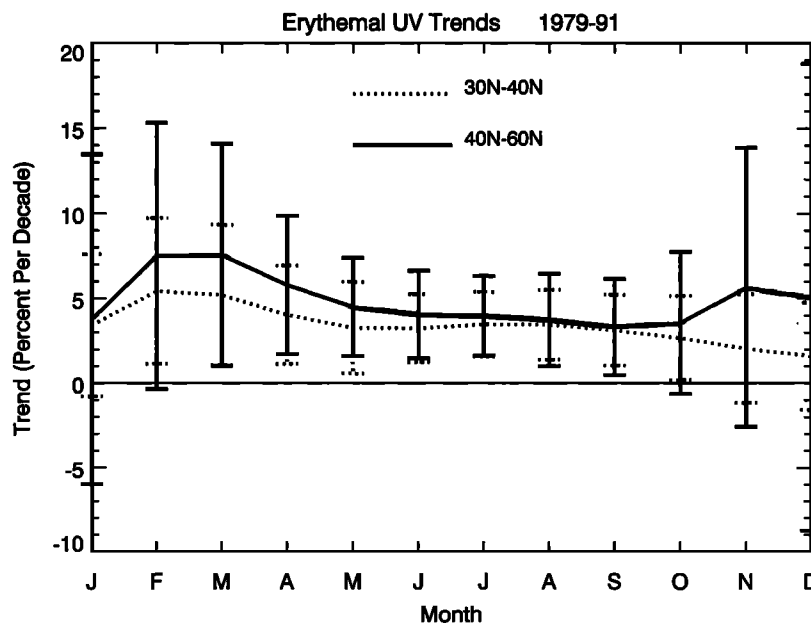


Figure 5. Seasonal trends in erythral UV zonal mean exposure data (units percent per decade) for 30° – 40° N (dotted) and 40° – 60° N (solid). Vertical bars denote $\pm 2\sigma$ uncertainties in trend coefficients.

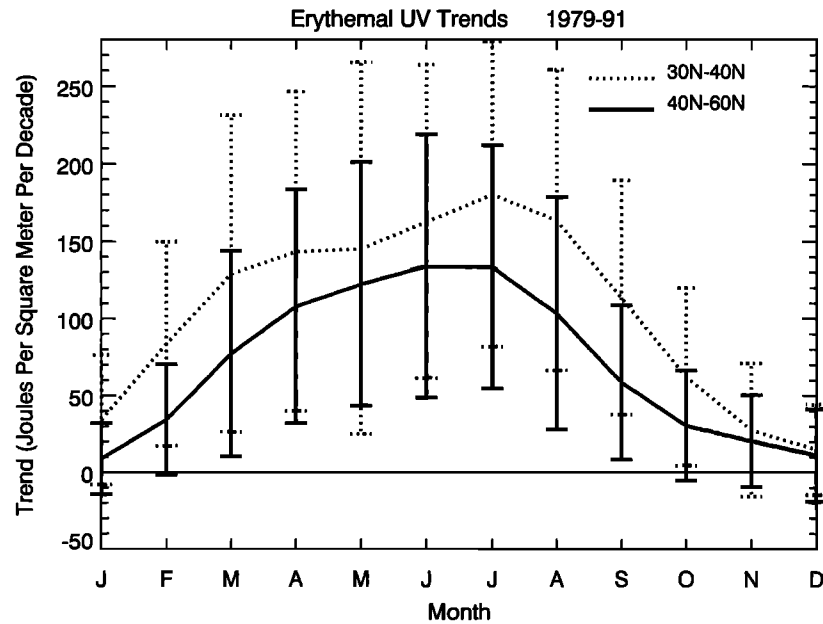


Figure 6. Seasonal trends in erythemal UV zonal-mean exposure data (units J m^{-2}) for 30° – 40°N (dotted) and 40° – 60°N (solid). Vertical bars denote $\pm 2\sigma$ uncertainties in trend coefficients.

continent in high latitudes indicate increases exceeding $+10\%$ per decade for the months of May–August. The important conclusion is that positive trends in the subtropical latitudes originate mostly over oceanic regions, whereas positive trends

at higher latitudes originate mostly over landmasses. Some of these increases in erythemal UV over central Europe and the east Asian continent can be attributed to decadal decreases in cloudiness.

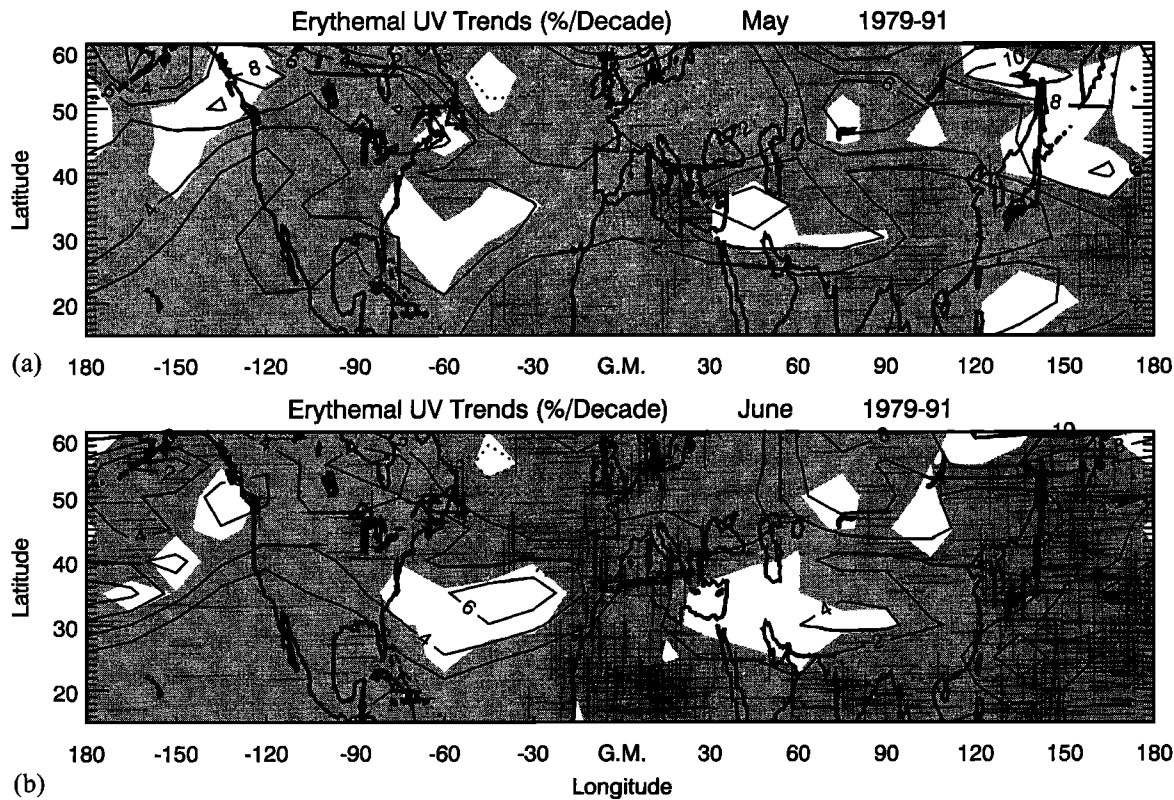


Figure 7. Northern Hemisphere latitude versus longitude 1979–1991 trends (units percent per decade) for (a) May and (b) June. Shading indicates trends not different from zero at the 2σ level.

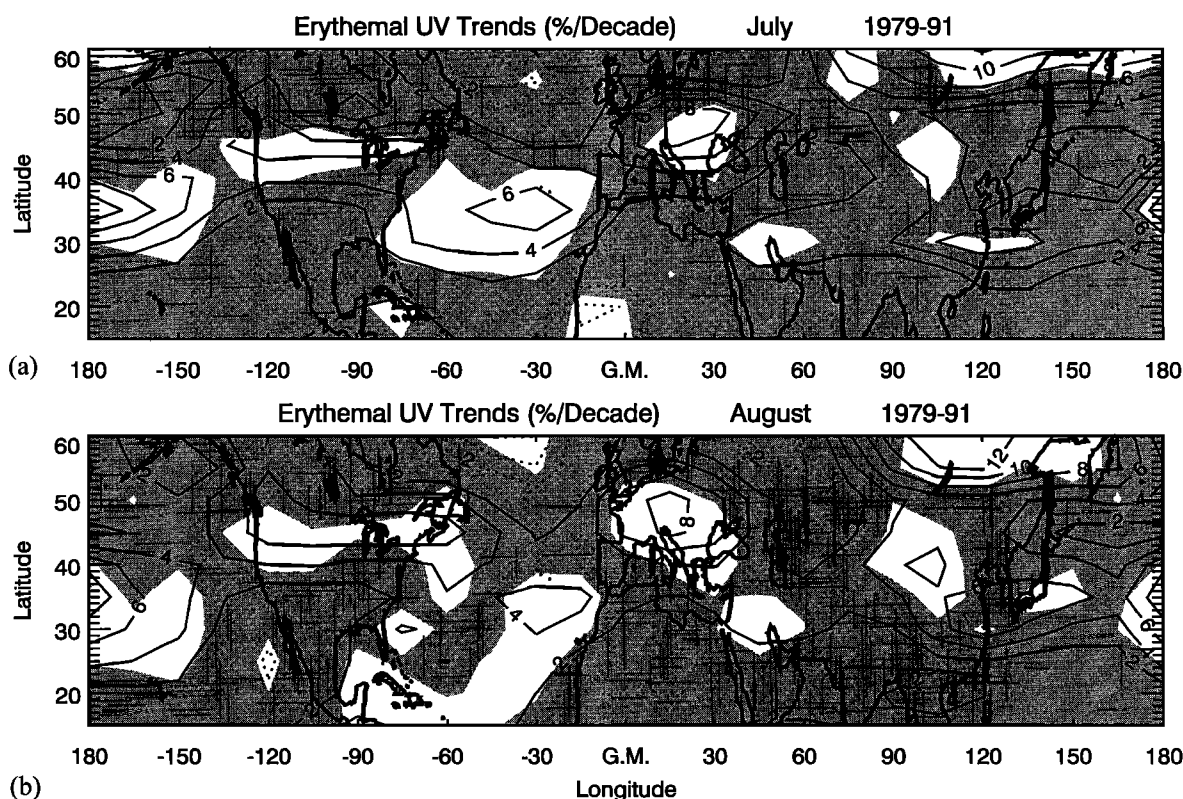


Figure 8. Northern Hemisphere latitude versus longitude 1979–1991 trends (units percent per decade) for (a) July and (b) August. Shading indicates trends not different from zero at the 2σ level.

Acknowledgments. We wish to thank members of the NASA TOMS Nimbus Experiment and Information Processing Teams for providing the version 7 TOMS ozone data and a special thanks to E. Celarier and N. Krotkov for their extensive contributions in the production of the erythemal UV data set. We also greatly thank NOAA for providing MSU4 temperature data used in this study and the three anonymous reviewers for their constructive input in improving this manuscript.

References

- Blumthaler, M., and W. Ambach, Indication of increasing solar ultraviolet-B radiation flux in alpine regions, *Science*, **248**, 206–208, 1990.
- Bojkov, R. D., V. E. Fioletov, and S. B. Diaz, The relationship between solar UV irradiance and total ozone from observations over southern Argentina, *Geophys. Res. Lett.*, **22**, 1249–1252, 1995.
- Bruhl, C., and P. J. Crutzen, On the disproportionate role of tropospheric ozone as a filter against solar UV-B radiation, *Geophys. Res. Lett.*, **16**, 703–706, 1989.
- Chandra, S., Changes in stratospheric ozone and temperature due to the eruption of Mt. Pinatubo, *Geophys. Res. Lett.*, **20**, 33–36, 1993.
- Chandra, S., C. Varotsos, and L. E. Flynn, The midlatitude total ozone trends in the northern hemisphere, *Geophys. Res. Lett.*, **23**, 555–558, 1996.
- Eck, T. F., P. K. Bhartia, and J. B. Kerr, Satellite estimation of spectral UVB irradiance using TOMS derived ozone and reflectivity, *Geophys. Res. Lett.*, **22**, 611–614, 1995.
- Farman, J. C., B. G. Gardiner, and J. D. Shanklin, Large losses of total ozone in Antarctica reveal seasonal ClO_x/NO_x interaction, *Nature*, **315**, 207–210, 1985.
- Fioletov, V., J. Kerr, and D. Wardle, The relationship between total ozone and spectral UV irradiance from Brewer observations and its use for derivation of total ozone from UV measurements, *Geophys. Res. Lett.*, **24**, 2997–3000, 1997.
- Gleason, J., et al., Record low global ozone in 1992, *Science*, **260**, 523–525, 1993.
- Herman, J. R., P. K. Bhartia, J. Ziemke, Z. Ahmad, and D. Larko, UV-B increases (1979–1992) from decreases in total ozone, *Geophys. Res. Lett.*, **23**, 2117–2120, 1996.
- Herman, J. R., N. Krotkov, E. Celarier, D. Larko, and G. Labow, Distribution of UV radiation at the Earth's surface from TOMS-measured UV-backscattered radiances, *J. Geophys. Res.*, **104**, 12,059–12,076, 1999.
- Hood, L. L., and D. A. Zaff, Lower stratospheric stationary waves and the longitude dependence of ozone trends in winter, *J. Geophys. Res.*, **100**, 25,791–25,800, 1995.
- Hood, L. L., J. P. McCormack, and K. Labitzke, An investigation of dynamical contributions to midlatitude ozone trends in winter, *J. Geophys. Res.*, **102**, 13,079–13,093, 1997.
- Lubin, D., and E. H. Jensen, Effects of clouds and stratospheric ozone depletion on ultraviolet radiation changes, *Nature*, **377**, 710–713, 1995.
- Madronich, S., The atmosphere and UV-B radiation at ground level, in *Environmental UV Photobiology*, edited by A. R. Young et al., pp. 1–39, Plenum, New York, 1993.
- McCormack, J. P., and L. L. Hood, Modeling the spatial distribution of total ozone in northern hemisphere winter: 1979–1991, *J. Geophys. Res.*, **102**, 13,711–13,717, 1997.
- McKenzie, R. L., P. V. Johnston, M. Kotkamp, A. Bittar, and N. J. D. Hamlin, Solar ultraviolet spectroradiometry in New Zealand: Instrumentation and sample results from 1990, *Appl. Opt.*, **31**, 6501–6509, 1992.
- McKenzie, R. L., B. Connor, and G. Bodeker, Increased summertime UV radiation in New Zealand in response to ozone loss, *Science*, **285**, 1709–1711, 1999.
- Mote, P. W., J. R. Holton, and J. M. Wallace, Variability in total ozone associated with baroclinic waves, *J. Atmos. Sci.*, **48**, 1900–1903, 1991.
- Niu, X., J. E. Frederick, M. L. Stein, and G. C. Tiao, Trends in column ozone based on TOMS data: Dependence on month, latitude, and longitude, *J. Geophys. Res.*, **97**, 14,661–14,669, 1992.
- Randel, W. J., and J. B. Cobb, Coherent variations of monthly mean total ozone and lower stratospheric temperature, *J. Geophys. Res.*, **99**, 5433–5447, 1994.
- Rex, M., et al., In situ measurements of stratospheric ozone depletion

- rates in the Arctic Winter 1991/92: A Lagrangian approach, *J. Geophys. Res.*, **103**, 5843–5853, 1998.
- Salby, M. L., and P. F. Callaghan, Fluctuations of total ozone and their relationship to stratospheric air motions, *J. Geophys. Res.*, **98**, 2715–2727, 1993.
- Schoeberl, M. R., and A. J. Krueger, Medium scale disturbances in total ozone during southern hemisphere summer, *Bull. Am. Meteorol. Soc.*, **64**, 1358–1365, 1983.
- Schubert, S. D., and M.-J. Munteanu, An analysis of tropopause pressure and total ozone correlations, *Mon. Weather Rev.*, **116**, 569–582, 1988.
- Stratospheric Processes and Their Role in Climate (SPARC), Assessment of trends in the vertical distribution of ozone, in *WMO: Ozone Research and Monitoring Project Rep. 43*, World Meteorol. Organ., Geneva, 1998.
- Tsay, S., and K. Stamnes, Ultraviolet radiation in the Arctic: The impact of potential ozone depletions and cloud effects, *J. Geophys. Res.*, **97**, 7829–7840, 1992.
- Udelhofen, P. M., P. Gies, C. Roy, and W. J. Randel, Surface UV radiation over Australia, 1979–1992: Effects of ozone and cloud cover changes on variations of UV radiation, *J. Geophys. Res.*, **104**, 19,135–19,159, 1999.
- von der Gathen, P., et al., Observational evidence for chemical ozone depletion over the Arctic in winter 1991–92, *Nature*, **375**, 131–134, 1995.
- Zerefos, C., D. S. Balis, A. F. Bais, D. Gillotay, P. C. Simon, B. Mayer, and G. Seckmeyer, Variability of UV-B at four stations in Europe, *Geophys. Res. Lett.*, **24**, 1363–1366, 1997.
- Zerefos, C., C. Meleti, D. Balis, K. Tourpali, and A. F. Bais, Quasibiennial and longer-term changes in clear-sky UV-B solar irradiance, *Geophys. Res. Lett.*, **25**, 4345–4348, 1998.
- Ziemke, J. R., S. Chandra, and R. D. McPeters, Dynamical proxies of column ozone with applications to global trend models, *J. Geophys. Res.*, **102**, 6117–6129, 1997.

S. Chandra, Atmospheric Chemistry and Dynamics Branch, NASA Goddard Space Flight Center, Greenbelt, MD 20771. (chandra@chapman.gsfc.nasa.gov)

J. Herman, NASA Goddard Space Flight Center, Greenbelt, MD 20771. (herman@tparty.gsfc.nasa.gov)

C. Varotsos, Physics Department, Building V, University of Athens, Panepistimioupolis, Athens, Greece 15784. (kvarots@atlas.uoa.gr)

J. R. Ziemke, NASA Goddard Space Flight Center, Code 916, Building 33, Room E417, Greenbelt, MD 20771. (ziemke@jwocgy.gsfc.nasa.gov)

(Received February 24, 1999; revised November 10, 1999; accepted November 15, 1999.)